



Strengthening unreinforced masonry walls using natural hemp fibers

Reem Bitar^a, George Saad^{a,*}, Elie Awwad^b, Helmi El Khatib^a, Mounir Mabsout^a

^a Department of Civil and Environmental Engineering, American University of Beirut, P.O. Box: 11-0236, Riad El Solh, Beirut, 1107, Lebanon

^b Department of Civil Engineering, Scientific Research Center in Engineering, Faculty of Engineering II, Lebanese University, Roumieh, Lebanon

ARTICLE INFO

Keywords:

Masonry walls
Out-of-plane loading
Flexural strengthening
Natural fibers
Hemp

ABSTRACT

This paper presents an experimental setup to study the effectiveness of using natural hemp fibers for enhancing the out of plane flexural capacity of unreinforced masonry walls. Wall specimens are constructed using normal-weight hollow concrete masonry units, and then hemp fiber fabrics are externally applied for strengthening. Performance of the hemp reinforced wall units is gauged by examining the flexural capacity, ductility, and failure modes of the wall specimens. A sensitivity analysis is conducted to investigate the effects of different strengthening configurations on the capacity of strengthened wall sections. Experimental results show that both the flexural capacity and ductility of the walls increase with an increase in reinforcement ratio.

1. Introduction

Many existing unreinforced masonry (URM) buildings around the world are threatened to collapse when subjected to extreme loading conditions such as earthquakes, hurricanes, impact or blast loads. Although strengthening URM buildings against out-of-plane bending might not directly enhance their seismic performance, the strengthening process will help in avoiding the failure of the wall elements caused by seismic inertial forces. Over the last decades, structural strengthening techniques of existing buildings have been based on the use of Fiber-Reinforced Polymer (FRP) composites. Common strengthening composite materials include glass and carbon fiber-reinforced polymers (GFRP and CFRP) which enhance both flexural and shear capacity of masonry walls [1]. Studies show that the application of FRP largely improves the structural performance of masonry walls in terms of tensile strength and ductility [2]. However, the poor fire resistance, high cost, and environmental effects are some disadvantages associated with the use of these composite materials [3]. Moreover, the issue of sustainability of FRP composites is often ignored [4]. One proposed sustainable solution is the substitution of synthetic fibers with natural fibers for strengthening existing structures since these fibers exhibit relatively good mechanical properties [5].

Among the various natural fibers, sisal, bamboo, coir, and jute fibers, hemp fibers are of particular interest as these fibers exhibit a relatively good tensile strength as compared to other lignocellulosic fibers. Studies have shown that the mechanical properties of hemp fiber are similar to those of glass fiber; this makes them a suitable alternative for glass fibers

for strengthening existing structures [6]. Hemp is abundant in nature, does not require intensive care to grow, and is a waste material most of the time; thus, the hemp fiber production process is more eco-friendly than synthetic fibers [4]. Although natural fibers are already largely employed in many industrial applications, the use of natural fibers as strengthening materials in structural applications is hardly applied [7]. This is mainly attributed to the intrinsic variability in the mechanical properties of natural fibers and to durability concerns [8]. A quick literature review shows that the use of natural fibers in construction is largely limited to studying their concrete confinement effects. Yan et al. [9] investigated the compression and flexural performance of flax fiber tube encased coir fiber reinforced concrete composite. Coir fiber is used for internal strengthening of the concrete mix (coir inclusion in the cementitious matrix) while the flax fiber (FFRP) tube provides external confinement to the concrete cylinders. The test results showed that FFRP tube confinement enhanced the compressive strength and ductility of both plain concrete and coir reinforced concrete specimens. Moreover, while the inclusion of coir fibers in the cementitious mix had no effect on the confinement effectiveness, test results showed that it increases the ultimate compressive strength and the corresponding axial strain of the specimen. Yan et al. [10] also studied the bonding effects on the compressive behavior of flax fiber reinforced polymer-confined plain concrete and coir fiber reinforced concrete. In their study, Yan et al. considered three types of bond: concrete confined by flax fiber reinforced polymer tube (naturally bonded), flax fiber reinforced polymer tube with internal flax fiber reinforced polymer rings (mechanically bonded) and flax fiber reinforced polymer wrapping (adhesively

* Corresponding author.

E-mail address: george.saad@aub.edu.lb (G. Saad).

<https://doi.org/10.1016/j.job.2020.101253>

Received 19 March 2019; Received in revised form 4 February 2020; Accepted 5 February 2020

Available online 8 February 2020

2352-7102/© 2020 Elsevier Ltd. All rights reserved.

bonded). The study concluded that the percentage of the confinement effectiveness depends on the type of bond between the FRP material and concrete core [10]. Sen et al. [4] investigated the flexural behavior of sisal fabric reinforced polymer and compared it to the behavior of carbon and glass fabric reinforced polymer composite. Reinforced concrete beams were bonded externally with sisal fiber reinforced polymer (SFRP), carbon fiber reinforced polymer (CFRP), and glass fiber reinforced polymer (GFRP). The test variables were the nature of the fibers (sisal, carbon and glass) and the wrapping technique (no wrapping for control, full wrapping and strip wrapping i.e. only 50% of the total area was used for strengthening). It was concluded that SFRP strengthening of RC beams showed increase in its flexural strength and improvement in the load deflection behavior and also exhibited the highest amount of ductility and delayed the formation of cracks. The sisal fibers failed without rupture as was the case for carbon FRP and without de-bonding as was the case of glass FRP. The highest load carrying capacity was for the fully wrapped beams, then the strip wrapped beams and the members with the least load carrying capacity were the control beam with no strengthening. The load carrying capacity of the natural sisal was comparable to that of the synthetic material [4]. Recent research by Menna et al. [11] investigated using inorganic mortars combined with a hemp fiber composite grid for strengthening the in-plane response of masonry panels. In their study, Menna et al. focused on developing a strengthening mechanism for masonry walls using a low viscosity epoxy resin to saturate a bi-directional grid of dry hemp chords, and thus allowing the grid to be easily packaged for delivery to installation sites. The hemp fiber chord grid is then bonded to wall panels using pozzolanic mortar. In their experimental study, Menna et al. assessed the in plane shear strength enhancements achieved by the newly proposed strengthening mechanism and concluded that the improvements are comparable to those obtained using FRP meshes [11]. Fagone and Ranocchiai [12] experimentally investigated the out-of-plane behavior of masonry panels strengthened with CFRP sheets. They subjected the wall specimens to a four point bending loading scheme while positioning them vertically to avoid the effects of the self-weight on the test results. The analysis of the results focused on failure patterns considering both the number of CFRP layers used and their respective anchorage mechanism. The results show that single leaf reinforced specimens exhibited crack patterns mostly concentrated in their central portion and failed because of masonry compressive failure. Double leaf specimens mainly failed due to de-bonding of the reinforcement. While the use of a spike anchorage system didn't affect the failure mode of single leaf reinforced specimens, it led to an increase of the ultimate strength of doubly reinforced walls. Qamar et al. [13,14] studied that use of natural fibrous plaster for out-of-plane strengthening of mortar free interlocked masonry walls. They compared the performance of plastered walls using either sisal fibers or rice straws for reinforcement to plain plastered and un-plastered wall specimens. The study concluded that plain plastering increases the lateral elastic stiffness of walls by about 16 times and the addition of fibrous reinforcement to the plaster will improve the performance by 500% and 74% for 8 mm and 20 mm thick plasters, respectively. The improvements in performance were depicted in both strength and ductility limits.

This study aims at investigating the out-of-plane flexural strength of URM walls reinforced with externally applied natural hemp fiber fabric. Emphasis is placed on the load-deflection response of the wall specimens tested. Since little information exists on externally applied natural hemp fiber fabric on masonry walls, an attempt is made to explain the overall behavior of the wall specimens including crack patterns. The performance of the strengthening technique is determined by examining flexural capacity, ductility, and failure modes.

2. Experimental program

2.1. Test specimens

Five different wall configurations are tested to investigate the effects of the reinforcement ratio, number of hemp fiber layers, and inclusion of anchors on the behavior of masonry wall units in terms of flexural capacity, ductility, and failure mode. Two identical walls are tested within each configuration to ascertain the validity of the presented results. The first experimental configuration designated as control is un-strengthened and is used for benchmarking purposes. The walls of the other four sets are strengthened with different configurations of externally bonded bidirectional hemp fiber-epoxy composite. Walls labeled HS are strengthened using hemp fiber strips while walls H1, H2 and H3 are fully wrapped with hemp fibers. H1 and H2 walls are strengthened via one layer of hemp only while two layers are used to confine the H3 walls. The hemp fibers are not anchored for H1 walls. For walls of series HS, H2, and H3 the hemp fiber sheets were anchored at the terminating ends by installing extra fabric wrapped in a U-shape to the back of the wall. Although this kind of anchorage system is not very practical for existing structures, it has been chosen for this experimental procedure to study the effectiveness of anchors in avoiding premature de-bonding failure of the hemp fiber fabric at the ends of the wall test specimens. Fig. 1 presents the dimensions and details of the test walls for each configuration. The wall specimens were simply dimensioned to be somehow representative of actual URM systems while abiding by the testing facility limitations. Table 1 presents the experimental testing matrix. It includes the hemp fiber surface area ratio which is defined as the ratio of the surface area of hemp reinforcement to the surface area of the masonry wall.

All walls were constructed using locally available normal weight hollow concrete masonry units having dimensions of $400 \times 100 \times 200$ mm with a net block surface area of $21,472 \text{ mm}^2$. The dimensions of the walls were $630 \times 2,050$ mm and one block wide. Each wall specimen is 3 courses high without any type of reinforcement or grouting of the hollow blocks. The walls were constructed in running bond and the joints were finished flush with the outside of the masonry units. All specimens were cured for 28 days before the hemp fiber fabric reinforcement was applied.

2.2. Material properties

Laboratory tests were performed on individual masonry blocks, mortar cubes, masonry prisms, and hemp fabrics to estimate the mechanical characteristics of the materials used for the wall construction. In order to represent the same properties of the walls, all the tests were performed on the same day of the wall testing. The average compressive strength of individual masonry units was 15.4 MPa [15]. The average compressive strength of 50 mm mortar cubes was 47.3 MPa [16]. For the compressive strength of the masonry assemblage, three CMU prisms were tested and the average compressive strength was found to be 11.2 MPa [15,17]. The tensile strength of the bidirectional hemp fabric strips having dimensions of $25 \times 300 \times 1.2$ mm was tested using a UTM at a loading rate of 1 mm/min [17]. The test setup for the hemp fabrics is shown in Fig. 2. The average results of three repetitions of the tensile test of hemp fabrics are: an ultimate tensile strength of 34 MPa, a modulus of elasticity of 1.66 GPa, and an ultimate strain at rupture 0.0457. A two-component epoxy, Sikadur 300, was applied as a bonding agent between the masonry walls and the hemp fabric. The mechanical properties of the epoxy as supplied by the manufacturer are shown in Table 2.

2.3. Testing procedure

All wall specimens were monotonically loaded to failure under four point bending loading. Loading was applied to the test specimens by a

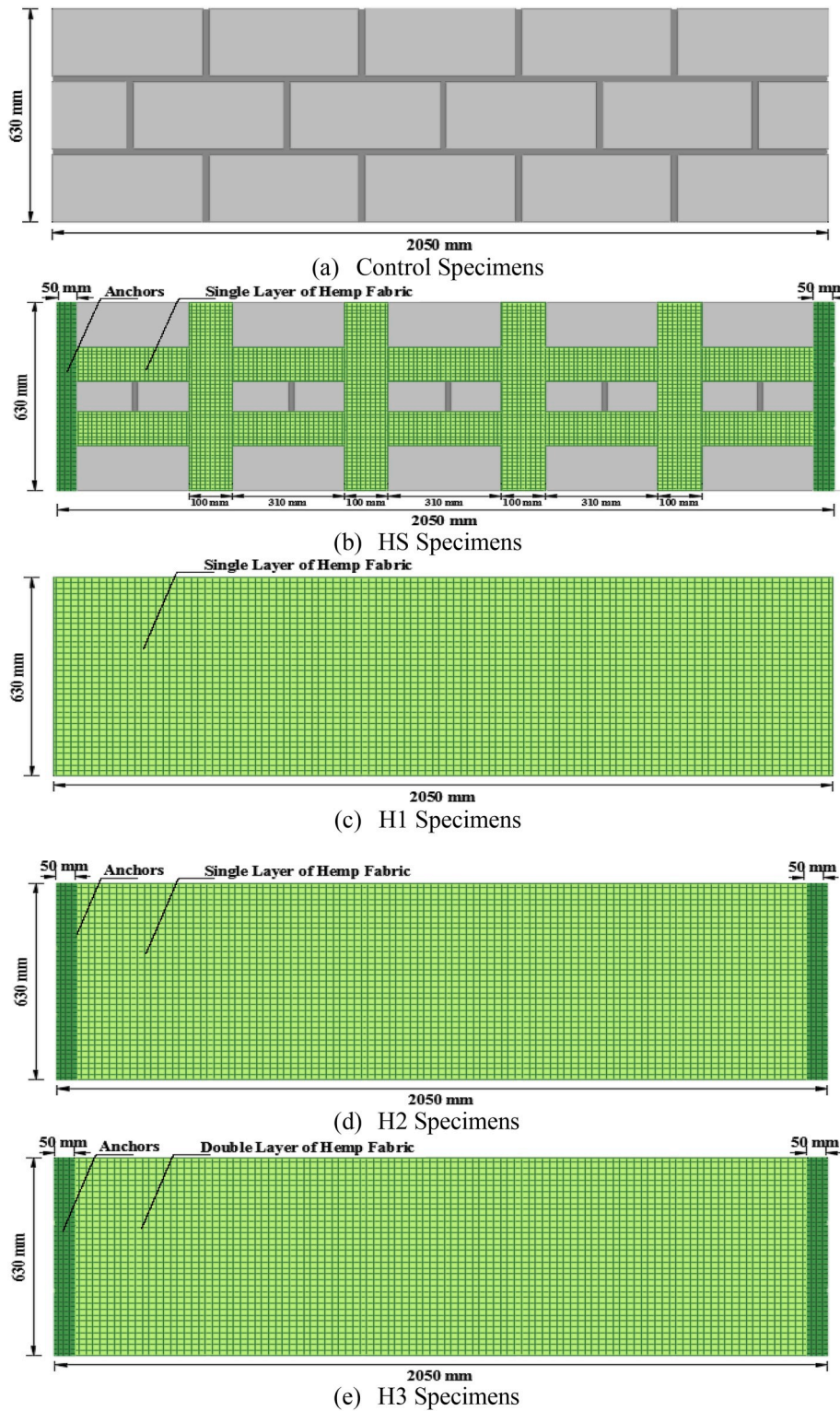


Fig. 1. Schematic representation of the different wall specimens.

hydraulic piston through two lines along the full width of the walls. The applied loading was measured electronically with a load cell having a capacity of 100 kN in compression. The instrumentation of the test setup consisted of various linear variable differential transducers (LVDT's) positioned on the compression side of the walls to measure deflections at the mid-span and near the two supports. Fig. 3 shows the test setup with the locations of LVDTs used for the test walls.

3. Analytical modelling

Section analysis is used to calculate the out-of-plane flexural capacity of un-strengthened and hemp fiber fabric-reinforced masonry walls.

3.1. Un-strengthened walls

The ultimate moment capacity of an un-strengthened control spec-

Table 1
Experimental testing matrix.

Series Name	Wall Identifier	Fiber Orientation	No. of Layers	No. of Strips	Reinforcement Ratio (%)	Surface Area Ratio (%)	No. of Specimens	Anchors
Control	C1	—	—	—	—	—	1	—
	C2	—	—	—	—	—	1	—
H S	HS-a	0°	1	2	0.381	51.3	1	Yes
		90°	1	4	—	—	1	Yes
	HS-b	0°	1	2	0.381	51.3	1	Yes
		90°	1	4	—	—	1	Yes
H 1	H1-a	0°	1	1	1.2	100.0	1	No
	H1-b	0°	1	1	1.2	100.0	1	No
H 2	H2-a	0°	1	1	1.2	100.0	1	Yes
	H2-b	0°	1	1	1.2	100.0	1	Yes
H 3	H3-a	0°	2	1	2	100.0	1	Yes
	H3-b	0°	2	1	2	100.0	1	Yes



Fig. 2. Tensile test setup of hemp fabrics.

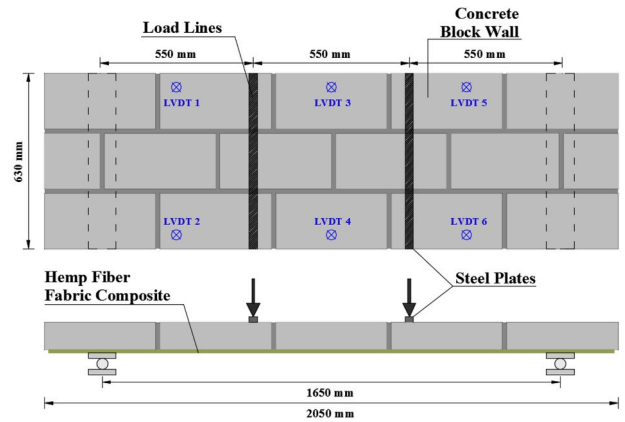


Fig. 3. Test setup and dimensions of the wall specimens, top and side views.

Masonry Standards Joint Committee (MSJC) [18].

3.2. Hemp-strengthened walls

The ultimate strength of hemp strengthened wall units should be derived as the minimum of the flexural and shear strengths of the composite cross-section. The derivation of the ultimate flexural strength of a hemp strengthened wall unit is via a simplified analytical method based on section equilibrium and strain compatibility with the following assumptions: (1) plane sections remain plane before and after bending, and strain in masonry and hemp fiber fabric shall be linearly proportional; (2) masonry does not exhibit any tensile strength; and (3) perfect bond between the hemp composite and the masonry is assumed, resulting in no relative slip between the two materials. Fig. 4 shows a free body diagram of the cross section of the hemp-strengthened masonry wall with the variation of strain and stress under out-of-plane loading. The strain is assumed to vary linearly along the height of the cross-section. Moreover, the strain in the extreme compression fiber is set equal to the maximum useable strain, ϵ_{mu} . The ultimate useable strain in the masonry at the top compression fiber was taken to be 0.0025 according to Section 9.3.2 of the MSJC code [19]. Above the neutral axis, the masonry compressive stress distribution was simplified and modeled as a rectangular uniform stress block with the maximum compression stress taken to be 80% of f'_M [19]. The stress block was taken to be located at a distance $a = 0.8c$ from the fiber of maximum compressive strain [19]. Referring to the stress diagram in Fig. 4, the compressive force resisted by masonry, C_M , and the tensile force of the hemp composite, T_f , were computed from:

$$C_M = 0.8 f'_M a w = 0.64 f'_M w c \tag{3}$$

$$T_f = A_f f'_{fu} = A_f \epsilon_{fu} E_f \tag{4}$$

imen is assumed to be dependent on the masonry's modulus of rupture f'_r . The modulus of rupture of concrete masonry units is assumed to be 10% of the minimum compressive strength of mortar, f'_m , obtained for mortar cubes, individual masonry units, and masonry prisms as follows:

$$f'_M = 0.1 \times \min(f'_{mortar}, f'_m(\text{units}), f'_m(\text{prisms})) \tag{1}$$

The cracking moment is then computed as:

$$M_u = M_{cr} = \frac{f'_r I}{y_t} = \frac{f'_r w t_m^2}{6} \tag{2}$$

where w and t_m are the width and thickness of the masonry wall, respectively.

For validation purposes, the cracking moment of the un-strengthened walls was also estimated in accordance with the

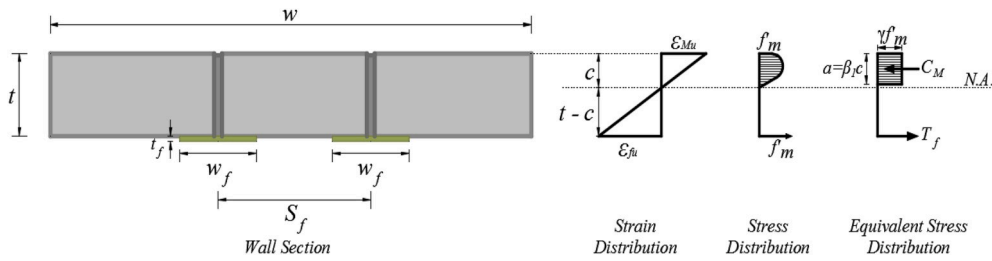


Fig. 4. Stress Strain distribution along the cross-section of a typical URM wall strengthened with hemp fiber fabric [20].

where w is the width of the wall; f'_M is the ultimate strength of masonry; f'_{fu} is the ultimate strength of the hemp composite; ϵ_{fu} is the hemp fiber fabric strain at ultimate stress; E_f is the Young's Modulus of the hemp fiber fabric; and A_f is the cross-sectional area of hemp composites given by:

$$A_f = n_s \times n_l \times w_f \times t_f \quad (5)$$

where, n_s is the number of hemp fabric strips applied to the wall; n_l is the number of hemp fabric layers; w_f is the width of hemp fabric strip; and t_f is the thickness per layer of hemp fabric composite. Based on the equilibrium of forces, the location of the neutral axis is determined as follows:

$$0.64 f'_M w c - A_f \epsilon_{fu} E_f = 0 \quad (6)$$

The ultimate flexural strength can then be determined from:

$$M_n = A_f \epsilon_{fu} E_f \left(t - \frac{0.8c}{2} \right) \quad (7)$$

or in terms of masonry compressive strength:

$$M_n = 0.64 f'_M c w \left(t - \frac{0.8c}{2} \right) \quad (8)$$

According to the MSJC [19], the derivation of the shear capacity of a URM wall unit shall be the minimum of: $1.5\sqrt{f'_M}$, 827kPa, and $413kPa + 0.45N_v/A_n$ where f'_M is the specified compressive strength of masonry A_n is the net cross-sectional area, and N_v is the compressive force acting normal to the shear surface. Moreover, MSJC uses the theoretical parabolic stress distribution rather than the average stress to calculate the shear stress. Therefore, the ultimate shear capacity of a masonry block unit having a net area of 21,472 mm² approximated as a rectangular cross-section ($V_{max} = \frac{3}{2} V/A$) for simplification is around 5.9 kN, and consequently the ultimate wall load capacity assuming four point bending should be around 11.8 kN. Since the cross-section is not rectangular, it is expected that the shear capacity should be around 14.8 kN assuming $V_{max} = 1.2V/A$. A detailed finite element analysis is required to calculate the exact stress multiplication factor which is beyond the scope of this study.

4. Experimental test results

4.1. Failure modes

Experimentally, failure of the wall specimen is defined as the point beyond which the wall can no longer sustain any increase in applied load. Table 3 lists each series of walls with its recorded mode of failure, and Table 4 presents the resulting fracture energy and ductility index of the different wall specimens. Fig. 5 depicts representative modes of failure of different tested wall series. For the control un-strengthened specimen, cracks initially appeared in the mortar head joints near the two line loads and then expanded laterally along the width of the wall. It was noted that the crack width increased with the increase of the load

Table 3
Summary of experimental results for tested specimens.

Series Name	Ultimate Load (kN)	Ultimate Midspan Deflection (mm)	Failure Mode
C	2.49	0.4015	Flexural Failure
H S	4.49	4.162	Hemp Rupture
H 1	10.72	16.47	Hemp Rupture
H 2	10.22	37.47	Hemp Rupture
H 3	16.3	73.68	Shear Failure

Table 4
Fracture energy and ductility index of the wall specimens.

Series	Reinforcement Ratio (%)	Fracture Energy (Nm)	Ductility Index
Control	—	0.5514	1
H S	0.381	12.625	22.89
H 1	1.2	162.25	294.25
H 2	1.2	326.48	592.1
H 3	2.0	1,014.1	1,839.1

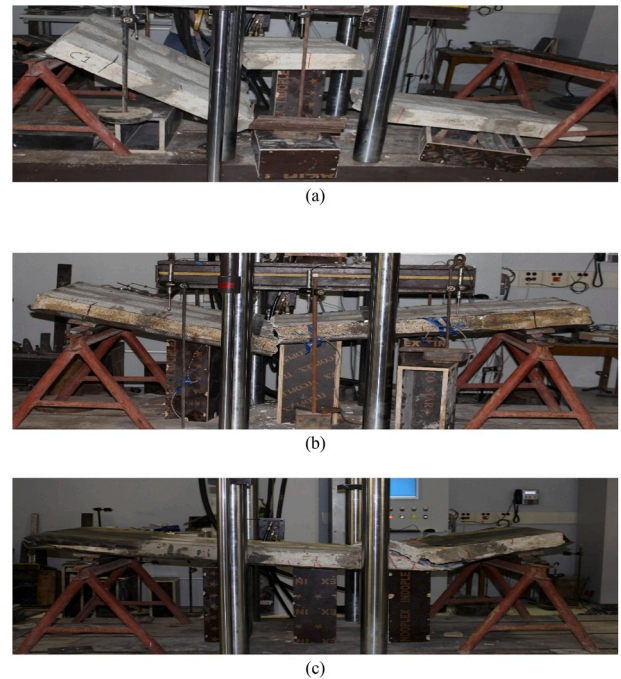


Fig. 5. Typical tested wall specimens: (a) Control Wall C1, (b) Wall H1-b, and (c) Wall H3-a.

which consequently led to the brittle failure of the wall at 2 locations, as shown in Fig. 5 (a). The failure of the control wall specimen occurred at a very low load, approximately 2.5 kN, and the measured mid-span deflection was only 0.6 mm. Two modes of failure were observed from all the strengthened wall specimens tested: (1) flexural rupture in the hemp fiber reinforcement (Walls HS, H1, and H2) and (2) shear failure of the wall near the support (Wall H3). No failure due to de-bonding between the hemp fiber reinforcement and the masonry units was observed in any of the wall specimens. For wall series (HS), (H1), and (H2), failure initiated by the development of micro-cracks in the masonry-mortar interface. As the load increased, cracks started to become visible in the mortar head joints and propagated along the bed joint, and the wall failed at the maximum moment region near the load line due to the rupture of the hemp reinforcement. The failure of wall series (H3), reinforced using two anchored layers of hemp fibers, was governed by shear failure. Failure initiated by the development of micro-cracks in the masonry-mortar interface. As the load increased, a series of flexural cracks started to become visible in the mortar head and bed joints in the maximum moment region. These cracks then expanded laterally along the width of the wall until failure. Shear failure in the blocks initiated underneath both loading points at the top of the wall and extended to the bottom side causing local de-bonding of the hemp reinforcement. The hemp reinforcement did not rupture nor did it de-bond anywhere else along the walls.

4.2. Load-deflection behavior

The load versus mid-span deflection curve is generally linear until one of the mortar joints loses its ability to carry the load and separates; consequently the wall fails in a brittle manner. To minimize the variability of the strengthened walls results, the load versus mid-span deflection curves of each series are averaged and the combined curves of all the series are shown in Fig. 6. The overall response of the strengthened walls can be separated into two stages. The first stage is almost linear which continues until achieving a mid-span deflection in the range of 0.7–1.2 mm. This phase ends when the tensile strength of the mortar between the joints reaches its limit and cracks initiate. As the bond between the mortar and any of the blocks is lost, a joint separates and the load is shifted to the subsequent connection. This is continued until all joints in the maximum moment region of the wall fail. At this point, the second stage which is a non-linear stage where large deflections begin to be registered for small increments of loads commences. At this stage, the mortar no longer contributes to the tensile capacity of the wall, and the hemp fiber layers become responsible for the flexural stiffness of the wall. During the second stage of loading, a change in the color of the hemp fibers is noticed, indicating the stretching that the material is undergoing. It is noteworthy from the

load-deflection curves that drastic drops as well as minor drops occur in the registered loads. The drastic drops indicate the development of new cracks in the wall, whereas the minor drops in loads indicate that the existing cracks were widening or spreading in depth. It is also noticed from the load-deflection curves that after each drop, the load recovers to a higher level but with a reduced stiffness.

Based on the LVDT readings, the deflection profiles of the walls along their length are plotted for one specimen of each series in Fig. 7. The plotted deflections correspond to the ultimate load carrying capacity for each specimen. The plots show how the deflection of the walls increased significantly with the increase in the reinforcement ratios of the wall in contrast to the very small deflection of the un-strengthened control wall. The ultimate mid-span deflection of the un-strengthened wall was only 0.4015 mm, while the ultimate mid-span deflections of the strengthened walls were 4.162, 16.47, 37.47, and 73.68 mm for series HS, H1, H2, and H3, respectively. Based on the results presented in Figs. 6 and 7, the effect of the anchorage is clearly noticed by comparing the load deflection/deflection profile curves for walls H1 and H2. This will be further discussed in a subsequent section on the ductility effects of the hemp fabric strengthening method.

4.3. Wall capacity

It is observed from the load-deflection responses that the out-of-plane strengths of masonry walls are increased significantly with the increased reinforcement ratio. The un-strengthened control wall specimen failed under a very low out of plane force with slight displacement. Fig. 8 plots the increase in the out-of-plane flexural strength of the wall specimens versus the hemp reinforcement ratio, ρ_f . As the hemp reinforcement ratio in wall series H1 and H2 is the same, their load capacities are averaged and the corresponding percent increase in out-of-plane capacity is computed. For the HS series with a hemp reinforcement ratio of 0.38%, the strengthening system provided 80% enhancement in the flexural strength of the wall compared to the control wall specimen. As ρ_f increased from 0.38 to 1.2%, an increase in the flexural strength of the wall from 80 to 320% as compared to the control specimen is noted. The further increase in ρ_f from 1.2 to 2.0%, for the H3 series, also resulted in a substantial enhancement in the moment capacity of the wall, which improved from 320 to 554% of that of the control specimen. Based on the plot presented in Fig. 8, it is noticed that an almost linear relationship exists between the hemp reinforcement ratio and the increase in the out of plane flexural strength of the walls.

4.4. Ductility index

To evaluate the ductility of the hemp-reinforced walls, a method based on the fracture energy, or absorbed energy, was used. Fracture

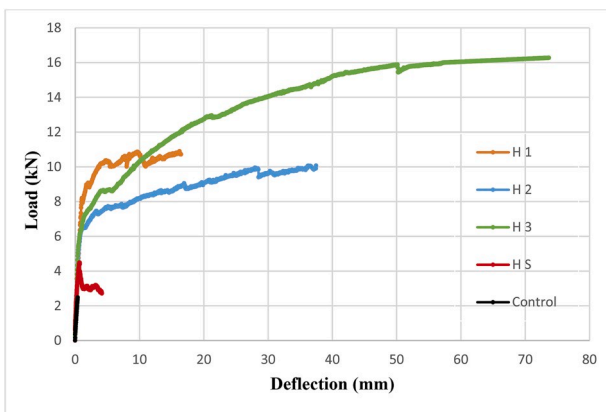


Fig. 6. Comparison of load-mid-span deflection response of all series (averaged).

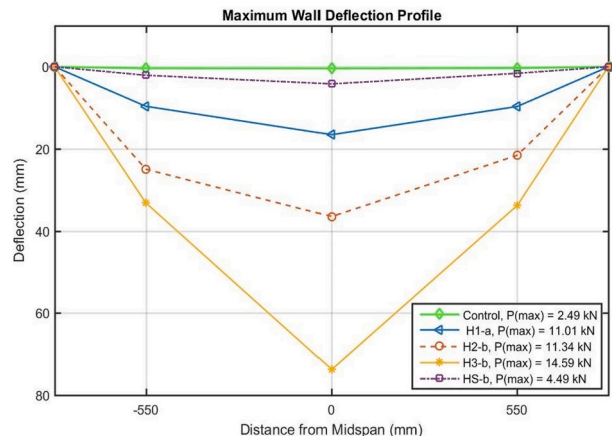


Fig. 7. Wall deflection profile at ultimate loads.

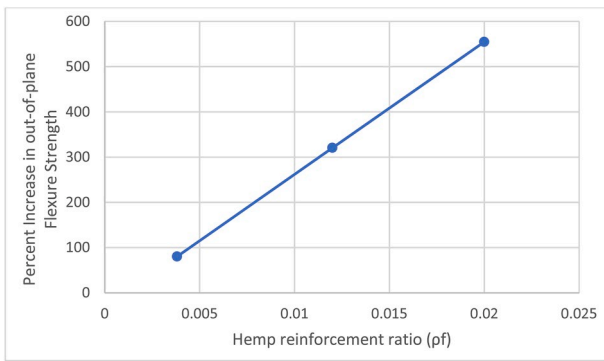


Fig. 8. Increase of flexural strength of retrofitted walls as a function of hemp reinforcement ratio.

energy is defined as the amount of energy absorbed by the specimen until it breaks. Having the load-deflection response, the total absorbed energy by the wall, its fracture energy, is simply given by the area under the curve. The ductility index which is the ratio of the fracture energy of a strengthened wall to fracture energy of the un-strengthened wall is used as a measure of the efficacy of hemp fabric strengthening. Fig. 4 shows the fracture energy and ductility indices of each of the wall series. The table results show that the ductility index increases with the increase of the reinforcement ratio. This indicates that the higher the reinforcement ratio the more energy is absorbed by the specimen and consequently more energy is needed to damage the specimen and rupture the hemp reinforcement layer. Moreover, although wall series H1 and H2 have the same reinforcement ratio, series H2 resulted in an increased ultimate mid-span deflection. Thus, the area under the load-displacement curve was larger than series H1 which explains the larger ductility index of series H2. Series H2 showed greater ductility due to the anchors provided at the ends of the wall. The gradual loss of bond between the anchors and the masonry before rupture of the hemp reinforcement resulted in a less brittle ultimate response and a slightly lower flexural capacity.

4.5. Performance of analytical model

4.5.1. Un-strengthened walls

The moment capacity of the control wall specimen was calculated using Equation (2). The modulus of rupture of masonry f'_r is assumed to be 10% of the minimum compressive strength identified from experimental testing as the average value of the masonry prisms with $f'_m = 11.2$ MPa. The moment capacity was calculated using both moduli and ultimate load results, which are shown in Table 5. Both the proposed and the MSJC methods underestimate the ultimate load capacity of the un-strengthened wall by 16% and 13%, respectively. However, both methods present a good and conservative estimate of the ultimate load capacity.

4.5.2. Hemp-strengthened walls

The capacity of the strengthened walls was calculated based on the proposed method presented in section 3.2 of this study. Equation (8) was used to compute the ultimate moment capacity for wall types HS, H1, and H2 since they all failed in flexure and the ultimate load was calculated and compared with the experimental ultimate load. Walls of type H3 failed in shear and consequently the shear capacity limit of 14.8 kN is assumed as the theoretical limiting load which is less than the

Table 5
Experimental and analytical results for un-strengthened wall.

Wall Identifier	Experimental Ultimate Load	Theoretical Ultimate Load	MSJC (2013)	Experimental/Theoretical	Experimental/MSJC
C1	2.49 kN	2.14 kN	2.19 kN	1.16	1.13

theoretical flexural capacity limit of the composite section calculated in accordance with equation (8) to be 15.9 kN. It should be noted that the computation of the ultimate capacities of the specimens did not include or consider the effect of the hemp anchorages on the ultimate capacity. Also, for series HS, the computation of the ultimate capacity included only the contribution of the hemp strips bonded parallel to the direction of bending and the effects of hemp strips bonded perpendicular to the direction of bending were ignored. The experimental to proposed ultimate capacity ratios are presented in Table 6. Table 6 shows that the presented model provides a good estimate of the load capacities of the hemp strengthened walls. Fig. 9 compares the experimental with the predicted ultimate failure loads for all specimens and shows that the predicted failures of strengthened and un-strengthened walls are conservative.

5. Conclusions

Experimental and analytical studies were performed on masonry-hemp reinforced walls, and the results were presented in this research. Accordingly, the following can be concluded:

- The overall response of the strengthened walls was similar and can be separated into two stages. The first stage is almost linear and characterizes the stiffness contribution of the masonry components of the walls. The second phase of the response was a non-linear stage which characterizes the stiffness contribution from the hemp fiber reinforcement.
- Externally bonded hemp fiber fabric composite systems substantially enhance the out-of-plane flexural capacity of unreinforced masonry walls. Experimental results show that the flexural capacity of the walls increases with the increase in the hemp reinforcement ratio. The increase in hemp reinforcement ratio to 2.0% led to a 554% increase in out-of-plane flexural strength when compared to the control unreinforced case.
- The hemp fiber fabric composites significantly increase the out-of-plane deflection capacity of URM walls. The experimental results highlight the importance of anchors in enhancing the ductility of the walls. This is especially evident when comparing the responses of the H1 and H2 wall series.
- The rupture of the hemp fibers was the most commonly observed failure mode of the strengthened specimens. Failure initiated by the development of micro-cracks in the masonry-mortar interface and as the load increased, cracks started to become visible in the mortar head joints at the maximum moment region and then the cracks laterally expanded along the width until failure.
- Shear failure governed the wall specimens strengthened with a reinforcement ratio of 2.0%. The hemp fiber fabric composite did not reach its ultimate tensile strength due to the high reinforcement ratio of the walls. This prevented the hemp fibers from rupturing while the

Table 6
Experimental and analytical results for hemp strengthened walls.

Series Name	Experimental Ultimate Load (kN)	Theoretical Ultimate Load (kN)	Experimental/Proposed
H S	4.49	3.26	1.37
H 1	10.72	9.90	1.08
H 2	10.22	9.90	1.03
H 3	16.3	14.8	1.10

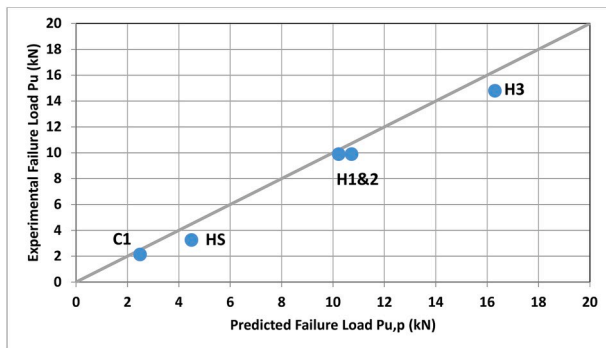


Fig. 9. Experimental failure load versus predicted load results.

masonry blocks of the walls reached their ultimate strength and failed in shear.

- Adding more layers of hemp fiber fabric composites to increase the reinforcement ratio would decrease the effectiveness of this strengthening technique in enhancing the flexural capacity and ductility of unreinforced masonry walls. Using a reinforcement ratio greater than 2.0% will result in significant reduction in the utilization of hemp fiber fabric composites and the strengthened wall loses its ductile behavior.
- In this study, an analytical predictive model for the ultimate load capacity was proposed for un-strengthened and strengthened walls. Results show that the proposed analytical model predictions underestimate the experimental ultimate load capacity of the un-strengthened wall by 16%. The predicted flexural capacities of the strengthened specimens resulted in 38, 8.3, 3.3, and 9% lower estimates than the average experimental results for series HS, H1, H2, and H3, respectively. The predicted ultimate load carrying capacities of both strengthened and un-strengthened walls are considered conservative.

CRedit authorship contribution statement

Reem Bitar: Investigation, Formal analysis, Writing - original draft.
George Saad: Conceptualization, Methodology, Supervision, Validation, Funding acquisition, Writing - review & editing.
Elie Awwad: Conceptualization, Methodology, Supervision, Validation, Funding acquisition.
Helmi El Khatib: Investigation, Supervision.
Mounir Mabsout: Conceptualization, Methodology, Supervision, Validation, Funding acquisition.

Acknowledgment

The authors are thankful to the Lebanese National Council for Scientific Research (LNCSR Project #22966) for the financial support, without which this research would not have been possible.

References

- [1] S. Pampanin, Controversial aspects in seismic assessment and retrofit of structures in modern times: understanding and implementing lessons from ancient heritage, *Bull. N. Z. Soc. Earthq. Eng.* 39 (2) (2006).
- [2] T. Triantafyllou, Strengthening of masonry structures using epoxy bonded FRP laminates, *J. Compos. Construct.* 2 (2) (1998) 96–104.
- [3] L. Bisby, M. Green, V. Kodur, Response to fire of concrete structures that incorporate FRP, *Prog. Struct. Eng. Mater.* 7 (3) (2005) 136–149.
- [4] T. Sen, H. Reddy, Application of sisal, bamboo, coir and jute natural composites in structural upgradation, *Int. J. Innovat. Manag. Technol.* 2 (3) (2011).
- [5] D. Asprone, M. Durante, A. Prota, G. Manfredi, Potential of structural pozzolanic matrix–hemp fiber grid composites, *Construction Building Materials* 25 (6) (2011) 2867–2874.
- [6] A. Shahzad, Hemp fiber and its composites – a review, *J. Compos. Mater.* 46 (8) (2011) 973–986.
- [7] O. Faruk, A. Bledzki, H. Fink, M. Sain, Progress report on natural fiber reinforced composites, *Macromol. Mater. Eng.* 299 (1) (2014) 9–26.
- [8] M. Minson, M. Islam, J. Epaarachchi, K. Lau, Analyses of woven hemp fabric characteristics for composite reinforcement, *Mater. Des.* 66 (2015) 82–92.
- [9] L. Yan, N. Chouw, Experimental study of flax FRP tube encased coir fibre reinforced concrete composite column, *Construct. Build. Mater.* (2013) 1118–1127.
- [10] L. Yan, A. Duchez, N. Chouw, Effect of bond on compressive behavior of flax fiber reinforced polymer tube-confined coir fiber reinforced concrete, *J. Reinforc. Plast. Compos.* 32 (4) (2013) 273–285.
- [11] C. Menna, D. Asprone, M. Durante, A. Zinno, A. Balsamo, A. Prota, Structural behaviour of masonry panels strengthened with an innovative hemp fibre composite grid, *J. Construct. Build. Mater.* 100 (2015) 111–121.
- [12] M. Fagone, G. Ranocchii, Experimental investigation on out-of-plane behavior of masonry panels strengthened with CFRP sheets, *Composites Part B* 150 (2018) 14–26.
- [13] F. Qamar, T. Thomas, M. Ali, Use of natural fibrous plaster for improving the out of plane lateral resistance of mortarless interlocked masonry walling, *Construct. Build. Mater.* 174 (2018) 320–329.
- [14] F. Qama, T. Thomas, M. Ali, Improvement in lateral resistance of mortar-free interlocking wall with plaster having natural fibres, *Construct. Build. Mater.* 234 (2020).
- [15] American Society for Testing and Materials, Standard Test Methods for Sampling and Testing Concrete Masonry Units and Related Units, 2015.
- [16] American Society for Testing and Materials, Standard Test Method for Compressive Strength of Hydraulic Cement Mortars, 2016.
- [17] American Society for Testing and Materials, Standard Test Method for Compressive Strength of Masonry Prisms, 2014.
- [18] American Society for Testing and Materials, Standard Test Method for Tensile Properties of Single Textile Fibers, 2014.
- [19] MSJC (Masonry Standards Joint Committee), Building Code Requirements for Masonry Structures, 2013.
- [20] H.M. Elsanadedy, Y. Al-Salloum, Z. Al-Zaheri, S. Alsayed, H. Abbas, *J. Compos. Construct.* 20 (6) (2016), 04016048.